Osteoarthritis and Cartilage Open 4 (2022) 100266

Contents lists available at ScienceDirect

Osteoarthritis and Cartilage Open

journal homepage: www.elsevier.com/journals/osteoarthritis-and-cartilage-open/2665-9131

Articular fragment restoration is critical to mitigate post-traumatic osteoarthritis in a porcine pilon fracture model

Graham J. DeKeyser [a], Richard Epperson [b,c], Chong Zhang [d], Dustin Williams [b,c], Aaron Olsen [e], Justin M. Haller [b,*]

[a] Department of Orthopedic Surgery, Harborview Medical Center, University of Washington, Seattle, WA, USA
[b] Department of Orthopedic Surgery, University of Utah, Salt Lake City, UT, USA
[c] Department of Veterans Affairs, Bone _ Biofilm Research Laboratory, Salt Lake City, UT, USA
[d] Department of Epidemiology, University of Utah, Salt Lake City, UT, USA
[e] Department of Animal, Dairy, and Veterinary Sciences, Utah State University, Logan UT, USA

ARTICLE INFO

Keywords:
Tibial plafond
Large animal model
Ankle arthritis
PTOA

ABSTRACT

Objective: During articular fracture reconstruction, orthopedic surgeons are frequently faced with the dilemma of retaining small articular fragments versus discarding these fragments. The purpose of this study was to compare post-traumatic osteoarthritis (PTOA) development between tibial plafond fractures and plafond fractures with a missing articular fragment (MF) in a porcine model.

Design: High-energy tibial plafond fractures in skeletally mature Yucatan mini pigs (n = 12) were created. During surgery, a 3 × 3 mm section of the articular surface was removed in six animals (MF group). Ankle synovial fluid was analyzed for IL-1β, IL-1Ra, IL-6, IL-8, and IL-10 concentrations obtained at initial surgery and 12 weeks post-surgery. Plafond and talus sections were evaluated for subchondral bone porosity and stained with Sanderson's Rapid Bone Stain and blindly evaluated to determine the Osteoarthritis Research Society International (OARSI) grade and vascular invasion.

Results: Fractured ankles had greater concentrations of IL-1β, IL-1Ra, IL-6, IL-8, and IL-10 compared to control ankles. There was no difference in cytokine concentrations between fractured and fractured + MF ankles. Fractured ankles had significantly greater bone porosity, vascular invasion, and OARSI grade as compared to the control group. In comparing tibial plafonds, the MF group had significantly more bone porosity, more vascular invasion, and a higher average OARSI grade than the anatomically reconstructed group. In comparing the talus, the MF group had higher average OARSI grade and similar bone porosity.

Conclusions: Articular fractures with a MF had worse PTOA development as measured by bone porosity, vascular invasion, and OARSI grade than the anatomically reconstructed fractures.

1. Introduction

Post traumatic osteoarthritis (PTOA) is a variant of osteoarthritis (OA) that occurs following an acute joint injury and is an increasing source of morbidity in active patients. While PTOA can develop following a variety of joint injuries, it most predictably occurs after intra-articular fracture (IAF). Approximately 12% of the 21 million patients in the United States with symptomatic OA can attribute their disease to PTOA [1]. Despite advances in healthcare and fracture management, the incidence of PTOA following IAF remains relatively unchanged over the last few decades [2].

Lower extremity IAFs result in some of the highest rates of PTOA. Studies show that 40% of patients with tibial plafond fractures develop PTOA at two years after injury and to 74% of patients progress to PTOA at a minimum of five years [3,4]. Even after three years from initial tibial plafond injury, patients continue to have poor outcomes that affect health and quality of life when compared to age-matched controls, and this often represents the start of a lifetime of impairment [5].

The mechanism(s) leading to injury progression from initial IAF to end-stage PTOA are unclear. The initial traumatic injury involves a complex process of articular displacement, ligamentous and supporting soft tissue disruption, and release of blood through the fracture into

* Corresponding author. University of Utah Department of Orthopaedic Surgery, 590 Wakara Way, Salt Lake City, UT, 84108, USA.
E-mail addresses: gjdekeys@uw.edu (G.J. DeKeyser), richardtepperson@yahoo.com (R. Epperson), chong.zhang@hsc.utah.edu (C. Zhang), dustin.williams@utah.edu (D. Williams), aaron.olsen@usu.edu (A. Olsen), justin.haller@hsc.utah.edu (J.M. Haller).

https://doi.org/10.1016/j.ocarto.2022.100266
Received 13 December 2021; Accepted 28 April 2022

injured joint space [6]. While articular reduction remains important to reduce joint contact stress, several long-term follow-up studies fail to demonstrate a clear relationship between anatomic articular reduction and diminished rates of PTOA [2,3,7]. Recently, two additional mechanisms for PTOA pathogenesis were proposed: 1) chondrocyte apoptosis and/or necrosis from the direct impact at the time of injury and 2) injury triggering a localized inflammatory response that exposes the articular cartilage to potentially harmful cytokines and proteases [2,8]. However, the impact of injury-related factors including articular comminution on PTOA development have not been investigated.

Orthopedic surgeons are commonly faced with the task of anatomically reconstructing articular fractures that have small or missing articular fragments. It is common practice for orthopedic surgeons to discard small fragments that are deemed non-reconstructable due to inability to adequately stabilize the pieces. However, it is not currently known how critical these fragments are to overall joint health and prevention of PTOA development. The purpose of the current study was to evaluate the importance of articular fragment reconstruction in PTOA development of the tibial plafond as measured by worsening histologic grade. The study hypothesis was that a missing articular fragment in anatomically reconstructed tibial plafond fractures leads to worse PTOA development in a porcine fracture model. Additionally, the study assessed the impact of a missing fragment on the histologic grade of the talus and synovial inflammatory cytokine concentrations in a tibial plafond fracture model.

2. Methods

2.1. Animal model

Following Institutional Animal Care and Use Committee (IACUC) approval, skeletally mature (mean age 37 months [range 17–56 months]) Yucatan mini pigs (Premier BioSource, Ramona California, USA) (mean weight 84.9 [range, 57–107 kg]) were used for the IAF model. All animal studies were reviewed and approved by the Institutional Animal Care and Use Committee at Utah State University, an AAALAC Accredited Institution. All research was conducted under protocol #10174. A custom impaction system was developed using compressed air to generate linear impaction into an anvil (Fig. 1A). Animals were anesthetized using a combination of ketamine (2.2 mg/kg), xylazine (2.2 mg/kg), telazol (4.4 mg/kg), and isoflurane (1–5%) and placed in a lateral position on the operating table using sterile conditions. Skeletal maturity was confirmed with fluoroscopy demonstrating closed distal tibial physis in all pigs (Fig. 1B). Porcine hindlimbs were connected to our impaction jig (Fig. 1A). In pilot testing of skeletally mature Yucatan mini pig hindlimbs, the anterior tibia cortical bone was too dense to create a consistent fracture using 70 J of energy. In order to create a consistent high-energy tibial plafond fracture, a medial incision over the anterior tibia was made and a sagittal saw was used to create a stress riser 2.5 cm proximal to the ankle joint. An impaction force (72 J) suitable to produce a high energy IAF was delivered with the impaction device. This system produced a displaced articular injury at the ankle with two large fragments and significant displacement (Fig. 1B). Adequate IAF was confirmed with fluoroscopy. The fractured ankle joint and contralateral control ankles were then aspirated 30 min after articular fracture. The synovial fluid was collected and set aside for biomarker analysis. For ankles with inadequate synovial fluid volume, 2 mL sterile saline was injected into the ankle and re-aspirated. The dilutional effect was normalized using serum blood urea nitrogen (BUN) relative to synovial fluid BUN as previously described [9]. Samples were processed using a centrifuge to separate out cellular debris and red blood cells, and the supernatant was frozen at −80 °C until subsequent analysis.

For the missing fragment (MF) group (n = 6), a 3 × 3 mm section of articular cartilage was removed from the tibial plafond. Specifically, the ankle joint capsule was incised along the fracture line and the anterior fracture fragment was externally rotated along its capsular and ligamentous attachments. A 3 × 3 mm section of only cartilage was surgically removed from along the fractured edge (Fig. 1C). For the anatomic fixation (AF) group (n = 6), the articular surface was not further disrupted after fracture. The tibial plafond fracture was then anatomically reduced and plated using a 3.5 mm stainless steel "T"-plate (Zimmer Biomet, Warsaw, IN) with 3.5 mm buttress screws (Osteocentric Technologies, Austin, TX) in the shaft and 2.7 mm lag screws through the plate perpendicular to the fracture (Fig. 1D). A cast was placed on the injured limb.

Animals were revived after fixation, placed in group housed facility with raised slatted floors in an American Association for Accreditation of

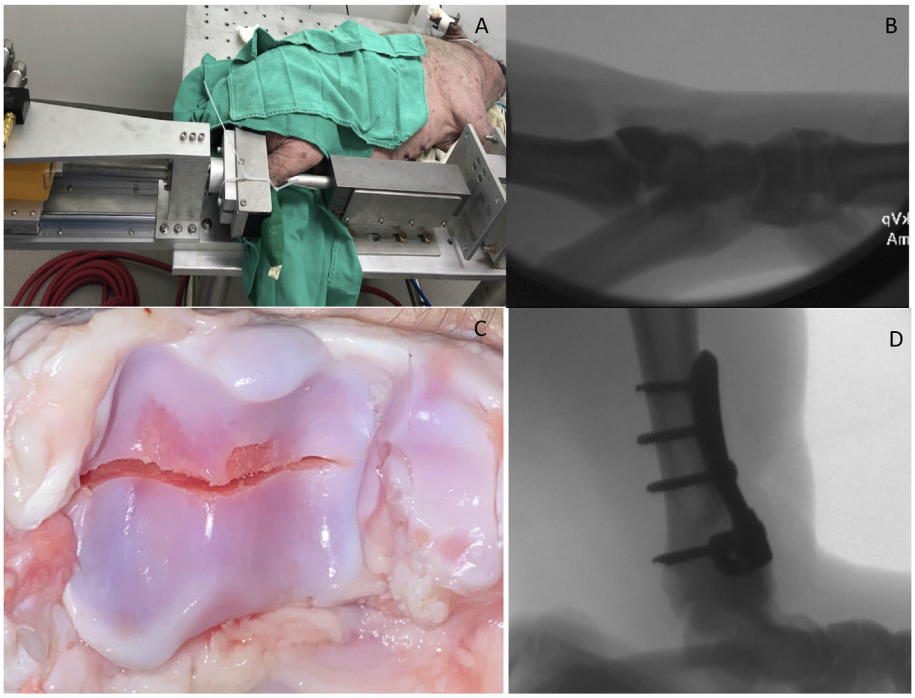

Fig. 1. (A)Representative photograph demonstrating the custom pneumatic actuator apparatus used to create the porcine tibial plafond fracture. (B) Representative fluoroscopic image demonstrating tibial plafond fracture. (C) Representative gross tibial plafond fracture created with custom fracture apparatus with 3 × 3 mm articular fragment removal. (D) Representative intra-operative lateral fluoroscopic image status post tibial plafond fracture creation and anatomic fixation with a 3.5 mm anterior plate with screws.

Laboratory Animal Care accredited facility. Animals were housed in a controlled environment with temperature maintained between 16 and 27 °C. Humidity was kept between 30 and 70% relative humidity, and light cycle was 12 h light and 12 h dark. Food and water was provided ad libitum with swine pellets purchased from a local agricultural supplier.

The pigs were monitored for pain, infection, and suffering, and administered analgesics and other care as required by professional veterinary personnel. During the 12-week study period, animals underwent anesthesia in order to undergo cast change at 1 week post-operatively.

We performed two separate injections of fluoro-label (tetracycline, 200 mg/ml (Bio-Mycin 200), Boehringer Ingelheim, Duluth, Georgia, USA) in order to label bone samples: one 16 days and one 5 days prior to euthanasia to create a double fluorescent label in the bone [10]. The double injections of tetracycline allowed for the assessment of bone viability and the ability to determine the rate at which the bone was remodeling in the subchondral region directly below the articular surface [11]. Animals underwent planned euthanasia to obtain final specimens at 12 weeks post injury.

2.2. Synovial fluid biomarker analysis

Synovial fluid samples were collected at 12-week necropsy and processed similar to the T_0 samples to quantify inflammatory cytokine concentrations. After all synovial fluid samples were collected, several inflammatory cytokines (IL-1β, IL1-Ra, IL-6, IL-8, and IL-10) were quantified using the Millipore Multiplex system (MilliporeSigma, Burlington, MA, United States) in triplicate. The assay utilizes antibodies linked to magnetic beads specific to each cytokine, and relative concentrations of each sample are analyzed compared to standard controls.

2.3. Radiography and Micro-CT

Following euthanasia, the distal portion of the hind limbs (repaired and contralateral) were harvested, disarticulated and dissected to remove any unnecessary soft tissue leaving only the distal tibia and tali. All specimens were radiographed for 3 min in a cabinet X-ray system set at 70 kV. In addition to radiography, Micro-CT scans (Quantum GX micro-CT (PerkinElmer; Waltham, MA.) were captured of the tali with a tube voltage of 90 kVp, tube current 180 μA, and a field-of-view (FOV) of 40 mm, which resulted in ~78 μm slices. The distal tibia samples could not be scanned due to the metal artifacts produced by the implanted hardware. The scans were 3D-rendered and analyzed using FIJI (Image J) software to observe any damaged to the articulating surface and to determine the porosity of the bone in a 5 mm region of interest (ROI) directly below the articulating surface (Fig. 2).

2.4. Histological processing

Pig ankles were fixed in 10% neutral buffered formalin for a minimum of 72 h and then placed into 70% ethanol. Small 3–5 mm sagittal sections were captured from the articular surface of both the tibiae and tali and included the entire tibial plafond with both the fracture and missing articular fragment area. Distilled water was dripped on the specimen while cutting to ensure the bone/tissue was not burnt due to excessive heat during sectioning. The small 3–5 mm sections from the articulating surface of the tibiae and tali were then decalcified, dehydrated and embedded in paraffin following standard techniques. 5 μm sections were created from each paraffin block and stained with Safranin O and Hematoxylin and Eosin (H&E) for light microscopy.

The remaining portion of the tibiae were dehydrated in ethanol, infiltrated, and embedded in PMMA using established techniques [11–13].The polymerized specimens were sectioned sagittally into 2–3 mm sections using a water-cooled saw equipped with a diamond-coated blade. The sections were ground and polished to optical finish using a variable-speed grinding wheel and coated with a conductive layer of carbon for approximately 30 s prior to scanning electron microcopy (SEM) imaging [11,13].

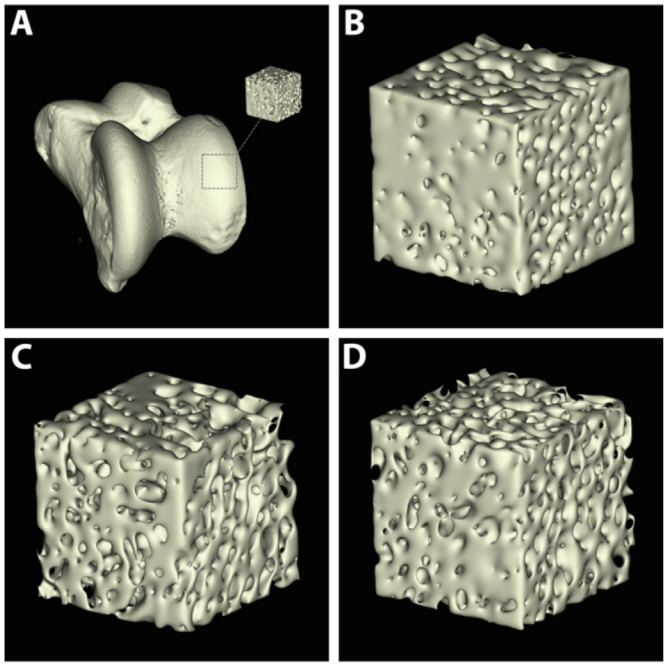

Fig. 2. (A) Three-dimensional reconstructed micro-CT scan of a talus from the control cohort demonstrating a 5 mm ROI being extracted directly below the articular surface for porosity analysis. (B–D) Representative 5 mm cubes from the control (B), AF (C), and MF (D) cohorts. Note the increased porosity in the AF and MF compared to the control.

2.5. Histological imaging _ analysis

Backscatter electron (BSE) imaging by SEM allowed for analysis of morphological components of bone damage, repair, mineralization and general activity. Digital BSE images were captured at ~20× magnification with a resolution of 2560 × 1920 pixels across the entire ankle. Post-image processing was done using Microsoft Research Image Composite Editor to mosaic/stitch the BSE images together, resulting in a high-resolution map of the entire ankle (Fig. 4) [14]. The SEM images were quantitatively measured for the percentage of bone in the subchondral region directly below the damaged cartilage and in the contralateral control ankle for host bone comparison. The BSE images were analyzed using a custom MATLAB program which uses grey level thresholding to measure the amount of bone versus pore space [11,15].

Following SEM imaging and analysis, specimens were ground to ~50 μm thickness and viewed under a mercury lamp microscope at a magnification of 200x to display the fluorochrome double-labeled bone. The double labels served two functions. First, the bone directly below the damaged cartilage was assessed for double or single fluorochrome labels. This confirmed whether the varying injury energy inhibited or advanced bone remodeling and confirmed whether the bone was still viable Next, the mineral apposition rate (MAR) was calculated in the subchondral region. This indicated if there was a regional acceleratory phenomenon in the due to the different treatment groups (Fig. 4) [11]. The MAR was calculated using the following equation:

$$MAR[\mu m / day] = \left[\sum x€(\pi / 4)\right] \Big/ nt$$

where $\sum x$ = sum of measurements between double labels, € = micrometer calibration factor (microns), π/4 = obliquity correction factor, n = number of measurements, t = time.

As noted above, the paraffin sections were stained with Safranin O and Hematoxylin and Eosin (H&E) while the PMMA sections were

stained with Sanderson's Rapid Bone Stain (SRBS) and Toluidine blue (Figs. 5 and 6). The stained sections were visually examined using a light microscope equipped with an image capturing software and graded using the Osteoarthritis Research Society International (OARSI) grade across the entire tibial plafond and talus [16]. As detailed by Goetz et al., the synovial fossa and fracture site complicates the analysis of the articular cartilage and cannot be accurately analyzed using the standard scale [17]. Therefore, the adjacent anterior and posterior regions of cartilage were graded and averaged into a single grade for each specimen. In addition to the OARSI grade, vascular invasion was calculated as number of vascular channels entering the subchondral bone, through the zone of calcified cartilage and into the deep layer of the articular cartilage per mm [18,19]. Histology and SEM assessments were performed by a bone pathology technician who was blinded to the experimental groups.

2.6. Statistical analysis

Statistical analysis was performed using R version 4.0.2 (R Core Team (2020). R: A language and environment for statistical computing. R Foundation for Statistical Computing, Vienna, Austria.URL https://www.R-project.org/.). Paired and un-paired two-tailed student's *t* tests were used for comparison between injured and control ankles, and between MF and AF treated ankles, respectively. P value < 0.05 was considered significant.

3. Results

3.1. Inflammatory cytokine analysis

Eleven of the 12 animals made it to the three-month endpoint. One animal in the MF cohort developed a post-operative infection and underwent early euthanasia. Inflammatory cytokine analysis at T_0 demonstrated significantly greater inflammatory response overall in the AF ankle as compared to the control ankle (Table 1). Similarly, cytokine analysis at T_0 demonstrated significantly greater inflammatory response in the MF ankle compared to the control ankle (Table 1). There was no difference in inflammatory response at T_0 between the AF and MF cohorts (IL-1β: 2.8 ng/mL vs. 2.9 ng/mL, p = 0.95; IL-1Ra: 3.0 ng/mL vs. 3.3 ng/mL, p = 0.80; IL-6: 1.8 ng/mL vs. 1.8 ng/mL, p = 0.98; IL-8: 0.1 ng/mL vs. 0.2 ng/mL, p = 0.34; IL-10: 9.3 ng/mL vs. 9.8, p = 0.91). At 12 weeks post-injury, the AF ankle and the MF ankle continued to have an overall significantly greater inflammatory response than the contralateral control ankle (Table 2). There was no difference in inflammatory response between the AF and MF cohorts at 12 weeks (IL-1β: 3.7 ng/mL vs. 2.3 ng/mL, p = 0.06; IL-1Ra: 4.8 ng/mL vs. 5.2 ng/mL, p = 0.89; IL-6: 2.5 ng/mL vs. 2.2 ng/mL, p = 0.78; IL-8: 0.1 ng/mL vs. 0.6 ng/mL, p = 0.25; IL-10: 11.8 ng/mL vs. 6.9, p = 0.09).

Table 1
T_0 synovial fluid inflammatory cytokine analysis.

Condition	Biomarker	Control (n = 5)	Injured (n = 5)	Difference (95%CI)	P value
AF	**IL-1β (ng/mL)**	0.18 (0.22)	2.79 (1.94)	2.62 (0.13,5.10)	0.043
	IL-1Ra (ng/mL)	0.17 (0.20)	2.96 (2.12)	2.79 (0.10,5.47)	0.045
	IL-6 (ng/mL)	0.03 (0.02)	1.85 (1.21)	1.82 (0.34,3.30)	0.027
	IL-8 (ng/mL)	0.01 (0.01)	0.15 (0.10)	0.14 (0.02,0.25)	0.032
	IL-10 (ng/mL)	0.05 (0.09)	9.26 (7.96)	9.21 (−0.71,19.13)	0.06
MF	**IL-1β (ng/mL)**	0.14 (0.24)	2.87 (1.51)	2.73 (1.02,4.45)	0.012
	IL-1Ra (ng/mL)	0.15 (0.26)	3.28 (1.83)	3.13 (1.06,5.20)	0.014
	IL-6 (ng/mL)	0.10 (0.11)	1.83 (1.09)	1.73 (0.42,3.04)	0.022
	IL-8 (ng/mL)	0.01 (0.01)	0.23 (0.16)	0.23 (0.03,0.42)	0.033
	IL-10 (ng/mL)	0.01 (0.01)	9.79 (5.75)	9.79 (2.65,16.92)	0.019

T_0- Time point zero (time of initial fixation); CI- Confidence interval; IL- Interleukin; ng/ML- Nanograms per milliliter; AF- Anatomic Fixation group; MF- Missing Articular Fragment group.

Table 2
T_{12} synovial fluid inflammatory cytokine analysis.

Condition	Biomarker	Control (n = 5)	Injured (n = 5)	Difference (95%CI)	P value
AF	**IL-1β (ng/mL)**	0.16 (0.20)	3.68 (1.31)	3.52 (2.02,5.03)	0.002
	IL-1Ra (ng/mL)	0.28 (0.38)	4.84 (1.21)	4.56 (3.47,5.65)	<0.001
	IL-6 (ng/mL)	0.15 (0.25)	2.46 (1.10)	2.32 (1.20,3.43)	0.003
	IL-8 (ng/mL)	0.01 (0.01)	0.06 (0.05)	0.06 (0.01,0.10)	0.022
	IL-10 (ng/mL)	0.07 (0.10)	11.76 (5.49)	11.69 (5.94,17.43)	0.003
MF	**IL-1β (ng/mL)**	0.14 (0.24)	2.27 (0.90)	2.13 (1.14,3.13)	0.004
	IL-1Ra (ng/mL)	0.02 (0.02)	5.15 (4.48)	5.13 (−0.44,10.70)	0.06
	IL-6 (ng/mL)	0.10 (0.11)	2.24 (1.36)	2.14 (0.48,3.81)	0.023
	IL-8 (ng/mL)	0.00 (0.01)	0.56 (0.82)	0.56 (−0.46,1.57)	0.20
	IL-10 (ng/mL)	0.10 (0.14)	6.95 (2.40)	6.85 (3.94,9.76)	0.003

T_{12}- Time point 12 weeks (12 weeks status post fixation); CI- Confidence interval; IL- Interleukin; ng/ML- Nanograms per milliliter; AF- Anatomic Fixation group; MF- Missing Articular Fragment group.

3.2. Subchondral bone

Qualitatively, the SEM BSE analysis revealed a more successful bony fusion at the fracture site and overall, greater surface continuity of calcified cartilage and subchondral bone in the tibial plafond AF cohort compared to the MF cohort (Fig. 4). Tibial plafond and talus subchondral bone porosity was compared between fractured and control samples as well as between AF and MF cohorts at 12 weeks post injury. Tibial plafond porosity (TPP) was significantly greater in the AF cohort as compared to control ankles (19.4% vs. 11.1.0%, p = 0.01). TPP was significantly greater in the MF cohort as compared to control ankles (35.1% vs. 10.4%, $p < 0.001$). TPP was significantly greater in the MF cohort as compared to the AF cohort (p = 0.001). Talus porosity was significantly greater in the AF cohort as compared to control ankles (36.2% vs. 26.0%, p = 0.02). Talus porosity was significantly greater in the MF cohort as compared to the control ankles (34.3% vs. 27.1%, p = 0.014). There was no difference in talus porosity between AF and MF cohorts (36.2% vs. 34.3%, p = 0.68).

Fluorochrome label analysis demonstrated an increase in labels, both single and double, directly below the articular surface of the tibiae in the AF an MF cohorts. This confirms the bone was still viable and actively remodeling following surgery and that the fracture and/or surgical procedure did not result in bone necrosis (Fig. 3). Both the AF (1.3 ± 0.3 μm/day) and MF (1.4 ± 0.3 μm/day) cohorts demonstrated a significant ($p < 0.001$) increase in the MAR compared to the control (0.7 ± 0.1 μm/day) cohorts confirming a regional acceleratory phenomenon (RAP) in the subchondral bone due to the fracture/repair. There was no difference in remodeling rate between the MF and AF cohorts at 12 weeks post-injury (p = 0.59).

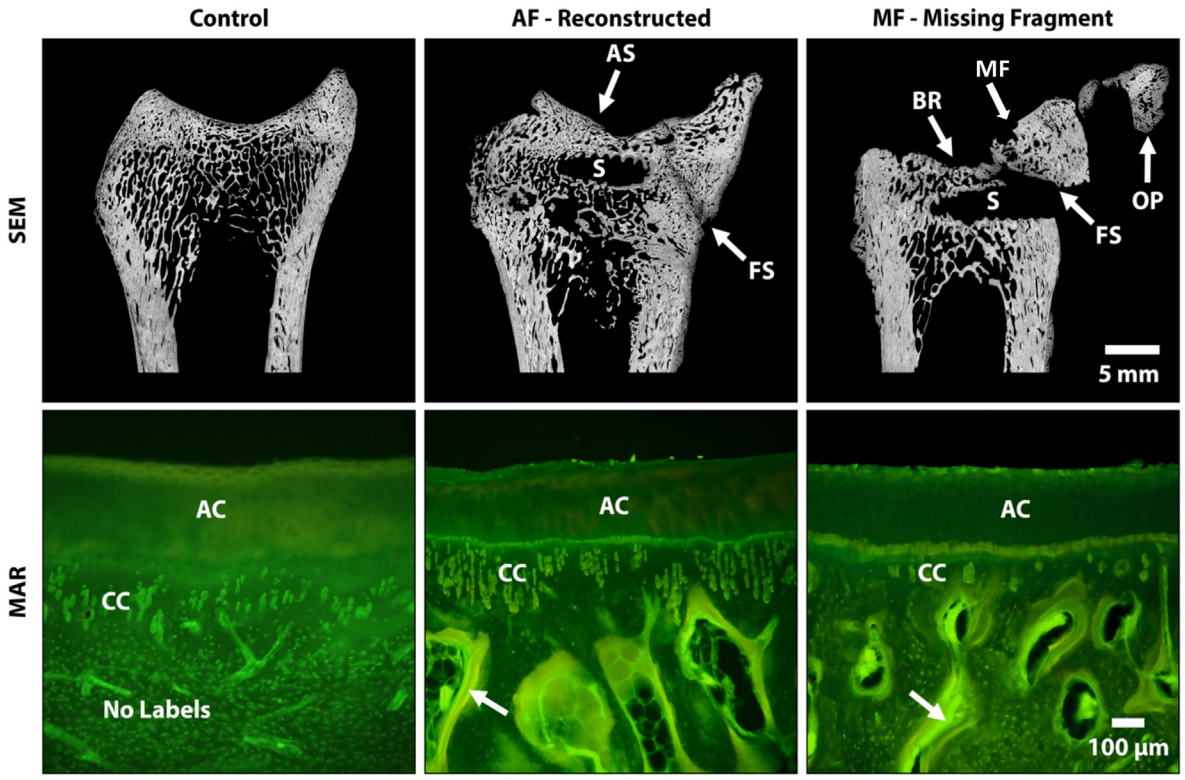

Fig. 3. Representative scanning electron microscopy images (Top) stitched together using Microsoft Research Image Composite Editor to create an overhead cross-sectional view of the tibiae. Grey = bone and Black = soft tissue/pore space. Note the modified articular surface (AS) due to bone resorption (BR), lack of bone fusion at the fusion site (FS) and possible osteophytes (OP) stemming from the anterior regions in the missing fragment (MF) (right image) sample. The black voids within the fractured samples are due to the removal of the surgical screw (S) and not bone resorption. Representative high power fluorochrome images (bottom) showing an increase in labels (arrows) directly below the articular and calcified cartilage (AC & CC) in the AF (middle) and MF (right) samples signaling a regional accelerated phenomenon.

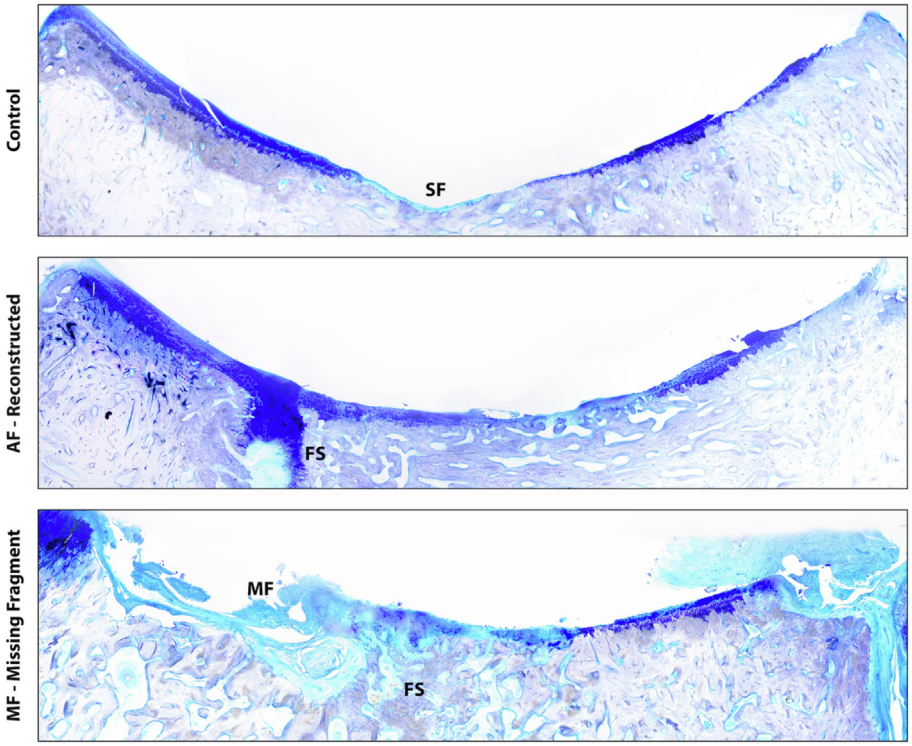

Fig. 4. Representative images of the distal tibia revealing that the missing fragment (MF) group demonstrated significantly worse PTOA with regional loss of the articular surface due to the MF compared to the anatomic fixation and control groups. FS=Fracture Site. SF=Synovial Fossa.

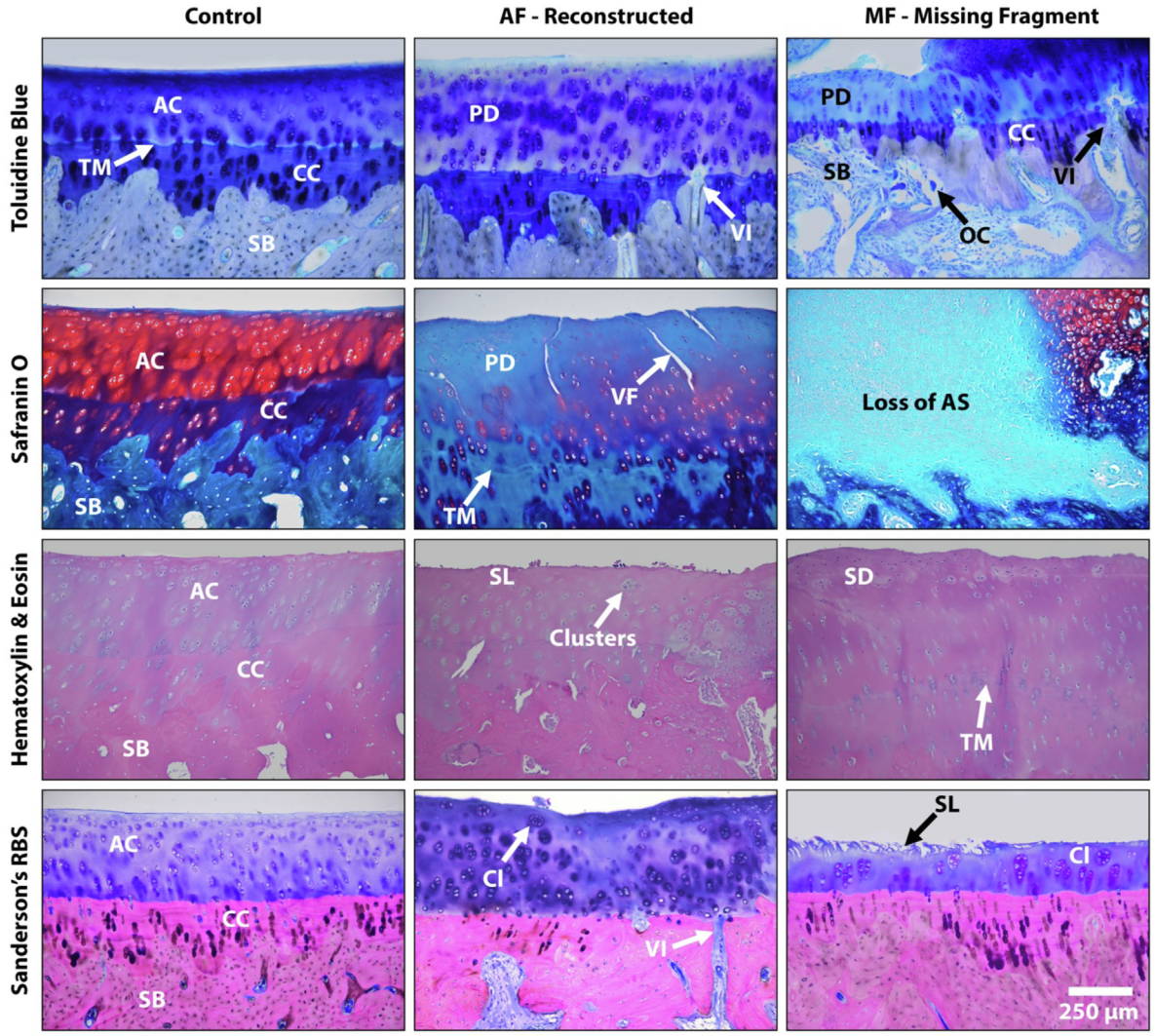

Fig. 5. Representative images of the distal tibia revealing that the missing fragment (MF) group demonstrated significantly worse PTOA with regional loss of the articular surface (AS), loss of subchondral bone (SB) by way of osteoclasts (OC) activity, proteoglycan depletion (PD), chondrocyte clustering (Cl), a loss of the superficial layer (SL), surface discontinuity (SD), modified/damaged regions of the calcified cartilage (CC), and a higher amount of vascular invasion (VI) compared to the anatomic fixation (AF) group. Specimens in both the AF and MF groups also demonstrated tide mark ™ duplication and vertical fissures (VF) in the articular cartilage (AC) in select regions.

3.3. Histologic analysis

Light microscopy analysis revealed that the AF cohorts followed a more standard trend of OA with chondrocyte clustering, proteoglycan depletion and vertical fissures. In contrast the MF cohorts displayed a more aggressive response, with a greater loss of articular cartilage, damaged superficial layer, osteoclast activity in the subchondral bone and an increase in irregular calcified cartilage structure (Figs. 4 and 5). The mean OARSI grade across the entire tibial plafond in the tibial plafond specimens were significantly greater in both the MF (OARSI = 3.8, range = 3–4.5) and AF (OARSI = 2.3, range = 1.5–3.5) as compared to control tibial plafond specimens (OARSI = 0.2, range = 0–0.5) ($p < 0.001$ and $p < 0.001$, respectively). The tibial plafond specimens from the MF cohort had significantly higher OARSI grade than the plafond specimens from the AF cohort ($p = 0.01$). Likewise, a significantly greater ($p = 0.0138$) amount of vascular invasions were observed in the MF cohort (1.1 ± 0.5/mm) compared to the AF cohort (0.5 ± 0.1/mm). Vascular invasion was not observed in the tibial plafond control cohorts.

Mean OARSI grade in talus specimens were also significantly greater for both the MF (OARSI = 4.4 range = 2–5, $p < 0.001$) and AF (OARSI = 2.2 range = 1–3.5, $p = 0.0029$) cohorts as compared to the control tali (OARSI grade 0.1 range = 0–0.5). The talus specimens from the MF cohort had a significantly greater OARSI grade than the talus specimens from the AF cohort ($p = 0.02$) (Fig. 6).

4. Discussion

Investigation into the pathogenesis of PTOA and potential therapeutics to mitigate PTOA development continues to evolve. Survivable large animal models are increasingly necessary in this process as they allow for realistic fracture creation, translatable surgical treatment, and have enough joint volume for targeted local injectables to modify the local response. The current study supported our hypothesis that a missing articular fragment in anatomically reconstructed tibial plafond fractures leads to worse PTOA development in a porcine fracture model. In this study, we describe a reproducible porcine tibial plafond fracture model that results in moderate PTOA for anatomically reduced fractures and significant PTOA for anatomically reduced fractures with a missing articular fragment (MF group) at three months post-injury.

The inflammatory cytokine concentrations were significantly elevated in the fractured ankles as compared to controls. Several previous animal fracture models of PTOA development demonstrate elevated

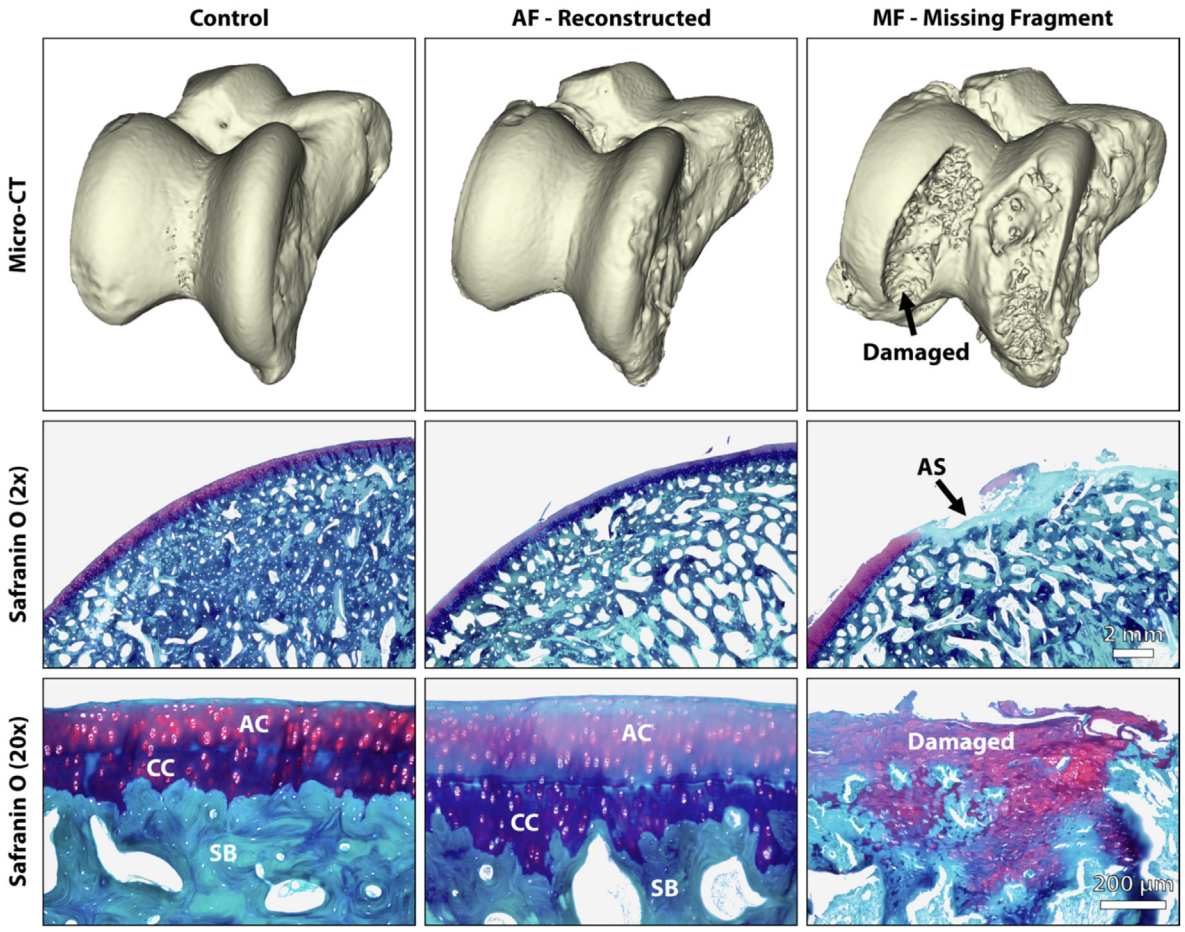

Fig. 6. Representative images of the talus demonstrating that the missing fragment (MF) in the reconstructed tibia resulted in severe damage to the articulating surface (AS) of the talus. The anatomic fixation (AF) group demonstrated that the majority of the articular cartilage (AC) and calcified cartilage (CC) remained intact with less signs of PTOA.

levels of synovial inflammatory cytokines [17,20–22]. Clinically, elevated inflammatory biomarker concentrations in the synovial fluid are reported in patients who sustain lower extremity articular fractures [23–25]. However, there was no difference in inflammatory response between the AF and MF groups. This could be related to using the same amount of energy to generate fracture in each group despite removing an articular fragment. Furman et al. demonstrated elevated proinflammatory cytokine concentrations acutely after fracture [22,26,27]. Goetz et al. demonstrated that inflammatory cytokine concentrations were acutely elevated in a porcine tibial plafond fracture and then returned to levels similar to controls by 12 weeks [17]. In this study, we observed synovial cytokine concentrations similar to Goetz et al. at one week, but the cytokine concentrations remained persistently elevated in the fracture groups by 12 weeks. The persistent elevation could be related to the presence of moderate to severe PTOA at 12 weeks that was not seen by Goetz et al. [17] Clinically, Adams et al. reported that patients with intra-articular ankle fracture continued to have elevated pro-inflammatory cytokine concentrations six months after injury [28].

We observed significantly worse PTOA development in the fracture groups compared to controls on both the tibial plafond and talus portions of the ankle. Furthermore, there was worse PTOA development on both the tibial plafond and talus portions of the ankle joint in the MF cohort as compared to the AF cohort. Similar to these findings, Coleman et al. demonstrated higher average Mankin scores in the talus and tibial plafond in a porcine tibial plafond fracture model compared to controls [29]. In this study, there was significantly greater vascular invasion in the MF group compared to the AF group and control ankles. Vascular invasion into the subchondral bone is associated with osteoarthritis development and progression [18].

Tibial plafond subchondral bone porosity was significantly higher in the MF group compared to the AF group. Subchondral porosity is identified as being associated with PTOA development and is thought to be related to increased osteoclast activity [30,31]. Furman et al. reported increased porosity following murine acute tibial plateau fractures that was associated with PTOA development. [22]The absence of an articular fragment did not affect the bone remodeling rate after a tibial plafond fracture as the MAR was similar between the MF and AF groups. However, the MF did result in a modified surface articular structure resulting in a more abrasive surface. The difference in PTOA severity in the anatomically reduced tibial plafond with a missing articular fragment group compared to the anatomically reduced tibial plafond group was striking.

In clinical practice, it is assumed that higher energy fractures create a higher rate of non-reconstructable, comminuted articular fragments, but the higher injury energy is the primary reason for PTOA development. However, the injury energy was the same between groups in this study, indicating that the difference in PTOA development is more related to the missing articular fragment. This finding is insightful as clinical and basic science trials of osteochondral lesions treated with a microfracture procedure demonstrate successful cartilage regeneration [32–35]. The exposed bone from the missing cartilage fragment may allow for blood or inflammatory cytokines that are present after fracture to persistently

leach into the joint and impede anabolic pathways in cartilage regeneration, leading to progressive cartilage degeneration [36]. Additional investigation into this process may be warranted to further understand why a missing articular fragment was associated with higher rates of ankle PTOA.

This study had several limitations. The study design ultimately created an osteotomy-assisted fracture model since an oscillating saw was used to cut the anterior tibial cortex. Pilot testing revealed that the tibial cortex of the skeletally mature Yucatan mini pigs was too dense to create a reproducible fracture with impaction only. There was additional joint manipulation in the MF cohort as compared to the anatomically reduced cohort, which could have an unintended impact on cartilage degeneration. However, all porcine surgeries were performed by an orthopedic trauma surgeon with meticulous attention to the capsular and vascular attachments on the anterior fracture fragment to minimize fragment devascularization. While the MF group received an anatomic reduction of the bone and most of the articular surface, a cartilage defect was created in this group (Fig. 1c) and this void could be considered non-anatomic. However, the vast majority of the entire articular surface was anatomically reduced. The tibial plafond fracture underwent fixation within 30 min of injury, which is much quicker than in clinical practice; clinically, tibial plafond fractures typically wait days to weeks to be definitively fixed with plates and screws. However, the immediate fixation did not seem to prevent PTOA development as both fracture groups demonstrated cartilage degeneration. Finally, the pigs were permitted immediate weight-bearing in a cast, which does not simulate common orthopedic practice. Immediate weight bearing could lead to a loss of reduction or subject the traumatized ankle cartilage to load prior to being sufficiently healed and lead to earlier PTOA development.

5. Conclusions

The authors present a viable, large animal fracture model that develops moderate to severe cartilage degeneration to study PTOA development. The current study demonstrates that ankle joints that have a missing articular fragment after tibial plafond fracture may be at higher risk of PTOA development as compared to fractures with an anatomically reconstructed articular surface. This may suggest that clinically, orthopedic surgeons should make every effort to retain and reconstruct articular fragments in order to mitigate PTOA development, while respecting the vascularity and soft tissue surrounding the fractured ankle. Treatment strategies such as osteochondral allograft or tissue-engineered chondral grafts may be necessary to mitigate missing articular fragments that are non-reconstructable in acute fractures to prevent PTOA development in patients with pilon fracture.

Author contributions

GD and JMH were primarily responsible for all sample and data collection, data analysis, study design, and manuscript writing. RE and DW conducted microCT analysis and processing, staining, and grading of histological sections. CZ performed statistical analysis and data interpretation. AO was responsible for study design, sample collection, and animal maintenance and care.

Funding source

LS Peery Foundation provided study support for study design, collection, analysis, and interpretation of data.

Declaration of competing interest

The authors declare no conflict of interest.

References

[1] T.D. Brown, R.C. Johnston, C.L. Saltzman, J.L. Marsh, J.A. Buckwalter, Posttraumatic osteoarthritis: a first estimate of incidence, prevalence, and burden of disease, J. Orthop. Trauma 20 (10) (2006) 739–744, https://doi.org/10.1097/01.bot.0000246468.80635.ef.
[2] M.L. Schenker, R.L. Mauck, J. Ahn, S. Mehta, Pathogenesis and prevention of posttraumatic osteoarthritis after intra-articular fracture, J. Am. Acad. Orthop. Surg. 22 (1) (2014) 20–28, https://doi.org/10.5435/jaaos-22-01-20.
[3] J.L. Marsh, D.P. Weigel, D.R. Dirschl, Tibial plafond fractures. How do these ankles function over time? J. Bone Jt. Surg. Am. Vol. 85-A (2) (2003) 287–295.
[4] A.M. Harris, B.M. Patterson, J.K. Sontich, H.A. Vallier, Results and outcomes after operative treatment of high-energy tibial plafond fractures, Foot Ankle Int./American Orthopaedic Foot and Ankle Society [and] Swiss Foot and Ankle Society 27 (4) (2006) 256–265.
[5] A.N. Pollak, M.L. McCarthy, R.S. Bess, J. Agel, M.F. Swiontkowski, Outcomes after treatment of high-energy tibial plafond fractures, J. Bone Jt. Surg. Am. Vol. 85-A (10) (2003) 1893–1900.
[6] D.R. Dirschl, J.L. Marsh, J.A. Buckwalter, et al., Articular fractures, J. Am. Acad. Orthop. Surg. 12 (6) (2004) 416–423.
[7] D.P. Weigel, J.L. Marsh, High-energy fractures of the tibial plateau. Knee function after longer follow-up, J. Bone Jt. Surg. Am. Vol. 84-A (9) (2002) 1541–1551.
[8] S.A. Olson, P. Horne, B. Furman, et al., The role of cytokines in posttraumatic arthritis, J. Am. Acad. Orthop. Surg. 22 (1) (2014) 29–37, https://doi.org/10.5435/jaaos-22-01-29.
[9] V.B. Kraus, T.V. Stabler, S.Y. Kong, G. Varju, G. McDaniel, Measurement of synovial fluid volume using urea, Osteoarthritis Cartilage 15 (10) (2007) 1217–1220, https://doi.org/10.1016/j.joca.2007.03.017.
[10] H.M. Frost, Tetracycline-based histological analysis of bone remodeling, Calcif. Tissue Res. 3 (3) (1969) 211–237.
[11] R.D. Bloebaum, B.M. Willie, B.S. Mitchell, A.A. Hofmann, Relationship between bone ingrowth, mineral apposition rate, and osteoblast activity, J. Biomed. Mater. Res. 81 (2) (2007) 505–514, https://doi.org/10.1002/jbm.a.31087.
[12] D.L. Williams, B.S. Haymond, J.P. Beck, et al., In vivo efficacy of a silicone–cationic steroid antimicrobial coating to prevent implant-related infection, Biomaterials 33 (33) (2012) 8641–8656, https://doi.org/10.1016/j.biomaterials.2012.08.003.
[13] D.L. Williams, B.S. Haymond, K.L. Woodbury, et al., Experimental model of biofilm implant-related osteomyelitis to test combination biomaterials using biofilms as initial inocula, J. Biomed. Mater. Res. 100 (7) (2012) 1888–1900, https://doi.org/10.1002/jbm.a.34123.
[14] R.T. Epperson, B.M. Isaacson, D.L. Rothberg, et al., Developing a combat-relevant translatable large animal model of heterotopic ossification, BoneKEy Rep. 15 (2021) 101127, https://doi.org/10.1016/j.bonr.2021.101127.
[15] R.T. Epperson, D. Mangiapani, R.D. Bloebaum, A.A. Hofmann, Bone ingrowth comparison of irregular titanium and cobalt-chromium coatings in a translational cancellous bone model, J. Biomed. Mater. Res. B Appl. Biomater. 108 (4) (2020) 1626–1635, https://doi.org/10.1002/jbm.b.34509.
[16] K.P.H. Pritzker, S. Gay, S.A. Jimenez, et al., Osteoarthritis cartilage histopathology: grading and staging, Osteoarthritis Cartilage 14 (1) (2006) 13–29, https://doi.org/10.1016/j.joca.2005.07.014.
[17] J.E. Goetz, D. Fredericks, E. Petersen, et al., A clinically realistic large animal model of intra-articular fracture that progresses to post-traumatic osteoarthritis, Osteoarthritis Cartilage/OARS, Osteoarthritis Research Society 23 (10) (2015) 1797–1805, https://doi.org/10.1016/j.joca.2015.05.022.
[18] M. Saito, T. Sasho, S. Yamaguchi, et al., Angiogenic activity of subchondral bone during the progression of osteoarthritis in a rabbit anterior cruciate ligament transection model, Osteoarthritis Cartilage 20 (12) (2012) 1574–1582, https://doi.org/10.1016/j.joca.2012.08.023.
[19] T.R. Oegema, R.J. Carpenter, F. Hofmeister, R.C. Thompson, The interaction of the zone of calcified cartilage and subchondral bone in osteoarthritis, Microsc. Res. Tech. 37 (4) (1997) 324–332, https://doi.org/10.1002/(sici)1097-0029(19970515)37:4<324::aid-jemt7>3.0.co;2-k.
[20] B.D. Ward, B.D. Furman, J.L. Huebner, V.B. Kraus, F. Guilak, S.A. Olson, Absence of posttraumatic arthritis following intraarticular fracture in the MRL/MpJ mouse, Arthritis Rheum. 58 (3) (2008) 744–753, https://doi.org/10.1002/art.23288.
[21] B.D. Furman, J. Strand, W.C. Hembree, B.D. Ward, F. Guilak, S.A. Olson, Joint degeneration following closed intraarticular fracture in the mouse knee: a model of posttraumatic arthritis, J. Orthop. Res. 25 (5) (2007) 578–592, https://doi.org/10.1002/jor.20331.
[22] B.D. Furman, D.S. Mangiapani, E. Zeitler, et al., Targeting pro-inflammatory cytokines following joint injury: acute intra-articular inhibition of interleukin-1 following knee injury prevents post-traumatic arthritis, Arthritis Res. Ther. 16 (3) (2014) R134, https://doi.org/10.1186/ar4591.
[23] J.M. Haller, M. McFadden, E.N. Kubiak, T.F. Higgins, Inflammatory cytokine response following acute tibial plateau fracture, J. Bone Jt. Surg. Am. Vol. 97 (6) (2015) 478–483, https://doi.org/10.2106/jbjs.n.00200.
[24] Haller JM, Marchand L, Rothberg DL, Kubiak EN, Higgins TF. Inflammatory cytokine response is greater in acute tibial plafond fractures than acute tibial plateau fractures. J. Orthop. Res.. Published online April 1, 2017. doi:10.1002/jor.23567.
[25] J.M. Haller, C.A. Swearingen, D. Partridge, M. McFadden, K. Thirunavukkarasu, T.F. Higgins, Intraarticular matrix metalloproteinases and aggrecan degradation are elevated after articular fracture, Clin. Orthop. Relat. Res. 473 (10) (2015) 3280–3288, https://doi.org/10.1007/s11999-015-4441-4.

[26] B.D. Furman, S.A. Olson, F. Guilak, The development of posttraumatic arthritis after articular fracture, J. Orthop. Trauma 20 (10) (2006) 719–725, https://doi.org/10.1097/01.bot.0000211160.05864.14.
[27] B.D. Furman, C.L. Kent, J.L. Huebner, et al., CXCL10 is upregulated in synovium and cartilage following articular fracture, J. Orthop. Res. 36 (4) (2018) 1220–1227, https://doi.org/10.1002/jor.23735.
[28] S.B. Adams, E.M. Leimer, L.A. Setton, et al., Inflammatory microenvironment persists after bone healing in intra-articular ankle fractures, *Foot Ankle Int./ American Orthopaedic Foot and Ankle Society [and] Swiss Foot and Ankle Society*. Published online January 1 (2017), https://doi.org/10.1177/1071100717690427, 1071100717690427.
[29] M.C. Coleman, J.E. Goetz, M.J. Brouillette, et al., Targeting mitochondrial responses to intra-articular fracture to prevent posttraumatic osteoarthritis, Sci. Transl. Med. 10 (427) (2018), eaan5372, https://doi.org/10.1126/scitranslmed.aan5372.
[30] H. Iijima, T. Aoyama, J. Tajino, et al., Subchondral plate porosity colocalizes with the point of mechanical load during ambulation in a rat knee model of post-traumatic osteoarthritis, Osteoarthritis Cartilage 24 (2) (2016) 354–363, https://doi.org/10.1016/j.joca.2015.09.001.
[31] S.M. Botter, G.J.V.M. van Osch, S. Clockaerts, J.H. Waarsing, H. Weinans, J.P.T.M. van Leeuwen, Osteoarthritis induction leads to early and temporal subchondral plate porosity in the tibial plateau of mice: an in vivo microfocal computed tomography study, Arthritis Rheum. 63 (9) (2011) 2690–2699, https://doi.org/10.1002/art.30307.
[32] D. Corr, J. Raikin, J. O'Neil, S. Raikin, Long-term outcomes of microfracture for treatment of osteochondral lesions of the talus, Foot Ankle Int. 42 (7) (2021) 833–840, https://doi.org/10.1177/1071100721995427.
[33] A.J. Krych, D.B.F. Saris, M.J. Stuart, B. Hacken, Cartilage injury in the knee: assessment and treatment options, J Am Acad Orthop Sur 28 (22) (2020) 914–922, https://doi.org/10.5435/jaaos-d-20-00266.
[34] S.W. Choi, G.W. Lee, K.B. Lee, Arthroscopic microfracture for osteochondral lesions of the talus: functional outcomes at a mean of 6.7 Years in 165 consecutive ankles, Am J Sports Medicine 48 (1) (2019) 153–158, https://doi.org/10.1177/0363546519887957.
[35] Han Q xin, Tong Y, Zhang L, et al. Comparative efficacy of osteochondral autologous transplantation and microfracture in the knee: an updated meta-analysis of randomized controlled trials. Arch Orthop Traum Su. Published online 2021:1-12. doi:10.1007/s00402-021-04075-9.
[36] L.P. Lyons, J.B. Weinberg, J. Wittstein, A.L. McNulty, Blood in the joint: effects of hemarthrosis on meniscus health and repair techniques, Osteoarthritis Cartilage 29 (4) (2020) 471–479, https://doi.org/10.1016/j.joca.2020.11.008.